Vanadium-Regulated Ultrafine Molybdenum Carbide Nanoparticles by Anchorage on Graphene for Highly Active Hydrogen Evolution Reaction

Xiuyong Yu*, Hao Liu and Shiduo Li
The first company of China eighth engineering division ltd, Jinan Shandong 250000, China.
1776375699@qq.com*

Summary: Platinum-like molybdenum carbide (Mo_2C) coupled with carbon-based supports is an effective strategy to promote the performance of catalysis and energy storage. However, inevitable aggregation of Mo_2C impede the achievement of high catalytic performance for hydrogen evolution reaction (HER). Herein, a vanadium-doped Mo_2C nanoparticles anchorage on graphene ($V-Mo_2C$) was developed. The V atoms can effectively regulate the electronic structure of Mo_2C, improving the intrinsic activity and kinetics of electrocatalyst for HER. The ultrafine Mo_2C nanoparticles with the size of about 2 nm are firmly anchorage on conductivity graphene substrate, which increases the number of active sites and contributes the high HER activity. As results, the $V-Mo_2C$ nanocomposite exhibits a remarkable HER performance with overpotentials of 284 mV at -10 $mA·cm^{-2}$ and corresponding Tafel slopes of 65.0 dec^{-1} in 1M KOH. Notable, the $V-Mo_2C$ hybrid is observed long term stability for > 24 h, demonstrating that the structure of Mo_2C nanoparticles anchored on graphene can significantly improve the performance for HER as well as stability. This work provides a reference for the synthesis of high-performance ultrafine transition metal carbide for HER or other catalytic system.

Keywords: Molybdenum carbide; Hydrogen evolution reaction; Vanadium doped; Ultrafine.

Introduction

Due to the energy crisis and environment pollution, it is necessary to find new green energy to replace the fossil fuels [1-3], which is very important for the aerospace, automotive and construction industries. Numbers of researchers focus their attention on hydrogen (H_2) due to its pollution-free and high energy density, which has been considered as a promising substitute [4-5]. The hydrogen evolution reaction (HER) is deemed to be a most optimal method to realize hydrogen generation [6-7]. Platinum, identified as the optimal HER electrocatalyst, is limited owing to its high cost and scarcity [6, 8-9]. Therefore, it is of great significance to explore efficient low cost and earth abundant noble metal free catalysts to replace Pt, which requires high active and long-term stability [10].

Currently, electrocatalysts based on transition metals (Ni, V, Mo, Fe and W) were reported, such as their oxides [11], carbides [12], sulfides [6, 13], nitrides [14], phosphides [15]. Among them, Pt-like molybdenum carbide (Mo_2C) is considered as promising candidate catalysts to replace noble Pt due to its special electronic structure, high excellent conductivity and pH applicability [1, 16-17]. However, it remains an enormously challenge to controllably minimize the particle size of Mo_2C and realize high specific surface areas synchronously due to inevitable aggregation and excessive growth of Mo_2C at high reaction temperature [18-19].

In view of previous studies, atoms doping is an effective method to regulate the electronic structure of catalysts. Electrocatalysts combining with carbon-based supports such as carbon nanotubes (CNTs) [20-21], graphene [22-23], and porous carbon [24-25] clearly demonstrated improvement in the dispersity of nanosized Mo_2C [26] and electron transport properties [27]. Graphene stands out among them due to large specific surface area and high conductivity, which is conducive to transportation of electrons and ions, further promoting catalytic activity [28].

Herein, we advanced a facile strategy to address these problems via V-doped and graphene anchoring. The V atoms can effectively tailor the electronic structure of Mo_2C, improving the intrinsic activity and kinetics of electrocatalyst for HER. The ultrafine Mo_2C nanoparticles with the size of about 2 nm are firmly anchoraged on conductivity graphene substrate, which increases the number of active sites and contributes the high HER activity. The as-prepared $V-Mo_2C$ demonstrates the relatively low overpotential in alkaline (η_{10} = 284 mV) solutions with favorable stability. The corresponding Tafel slopes was only 65.0 dec^{-1}. This work provides a facile and universal strategy for hybridizing ultrafine

---

transition metal carbide and carbon-based supports for effective hydrogen generation or other catalytic systems.

Experimental

Materials: Ammonium molybdate $((NH_4)_6Mo_7O_{24})$, ammonium metavanadate (NH_4VO_3), aniline, potassium hydroxide (KOH), anhydrous ethanol, hydrochloric acid (HCl), Pt/C (20 wt.% Pt on Vulcan XC-72R) were purchased from Sigma-Aldrich. Deionized water was used throughout all the experiments.

Synthesis of V-MoO₃: V doped MoO_3, denoted as V-MoO₃, was prepared by a simple polymerization process. Typically, 2 mmol $(NH_4)_6Mo_7O_{24}.4H_2O$ was dispersed in 36 mL of deionized water and stirred to form a homogeneous dispersion. 0.5 mmol NH_4VO_3 was then added into the homogeneous dispersion. Subsequently, 2 mL of aniline was added dropwise and stirred for 24 h. After the reaction, the sediments were collected and washed by distilled water and absolute ethanol for several times to remove any possible residue and dried in vacuum at 60°C for overnight.

Synthesis of V-Mo₂C: The synthesis method of Mo₂C is similar to the previous report [29]. 0.2 g V-MoO₃, 0.4 g $NaHCO_3$ (carbon source), and 0.2 g Mg powders were mixed and heated at 700 °C for 5 h and then cooled to room temperature in a tube furnace filled with Ar. The product was washed with 3 M HCl to remove the MgO, and vacuum dried at 80 °C overnight. Mo₂C was prepared by the similar process except that adding NH_4VO_3.
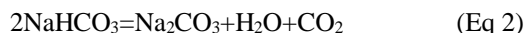
Materials Characterizations: The phases composition of the samples was investigated using X-ray diffraction (XRD) with Cu Kα radiation (λ=1.5406 Å) at a scanning step of 5° min⁻¹. The morphology and microstructure of the samples were studied by scanning electron microscopy (SEM) and transmission electron microscopy (TEM) equipped with an Oxford energy-dispersive X-ray spectrometer (EDS). X-ray photoelectron spectroscopy (XPS) analysis was operated using a Thermo fisher Scientific K-Alpha+ system.

Electrochemical Measurements: All electrochemical measurements were performed with a three-electrode system using Gamry Interface 1000 electrochemical workstation.

A carbon rod was used as the counter electrode, and Ag/AgCl electrode (E^0 = 0.198 V) was used as the reference electrode. As for working electrode, 10 mg of catalysts or 20 wt.% Pt/C were ultrasonically dispersed in the mixture containing 500 μL ethanol, 480 μL water, and 20 μL Nafion solution (10 wt.%) to form homogenous catalyst ink. 5 μL of the catalyst ink was then dipped on a polished glass carbon electrode (GC, Ø 3 mm) and dried in air. To characterize the electrocatalytic activity, the LSV curves were conducted in 1M KOH with a scan rate of 5 mV s⁻¹. The Tafel slopes were calculated based on the equation: η= b log (j) + a, Where η, a, b and j were denoted as the overpotential, Tafel constant, the Tafel slopee and the current density, respectively. EIS was performed with frequencies from 0.1 to 100000 Hz and an amplitude of 10 mV. The stability test was conducted at -0.284 V_{RHE} for 20 h.

Results and discussion

X-ray diffraction (XRD) was measured to investigate the crystal structure and composition of V-Mo₂C catalyst. The typical peaks at 34.3°, 38.0°, 39.4°, 52.1°, 61.5°, 69.6°, and 74.6°, being assigned to (100), (002), (101), (102), (110), (103), and (112) planes of Mo₂C, as shown in Fig. 1a. The typical diffraction peak locating at 26.0° is assigned to C (002). The XRD results indicate that the Mo₂C particles were sucessfully prepared. The reactions in magnesium thermal reaction are demostrated as follows:
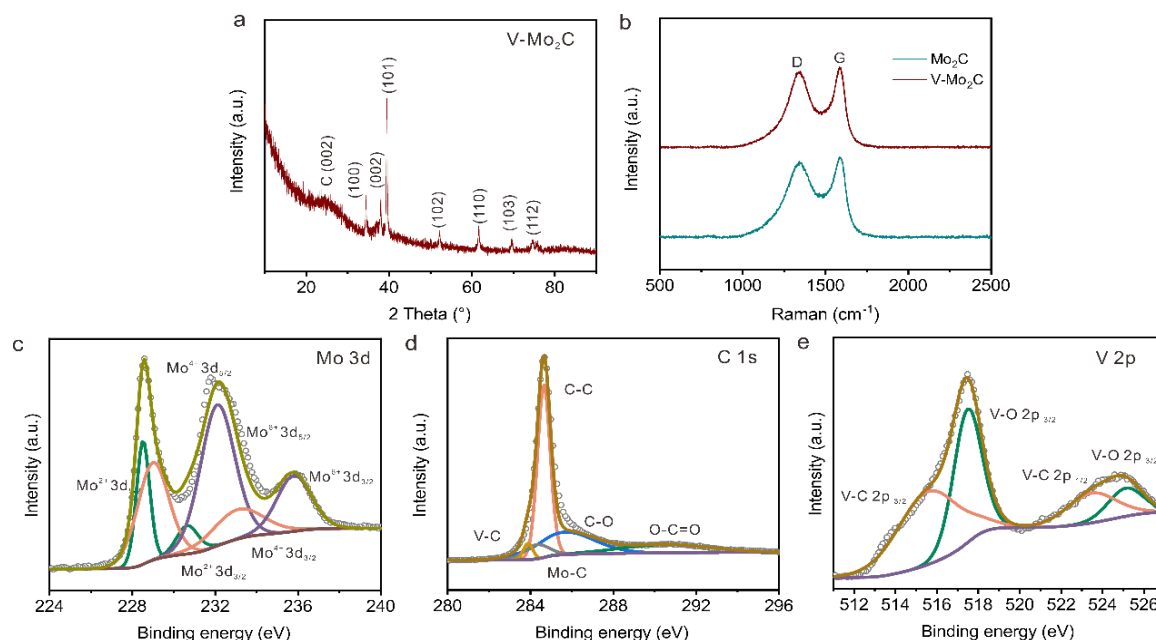
$3Mg + MoO_3 = 3MgO + Mo$	(Eq 1)
$2NaHCO_3 = Na_2CO_3 + H_2O + CO_2$	(Eq 2)
$2Mg + CO_2 = 2MgO + C$	(Eq 3)
$2Mo + C = Mo_2C$	(Eq 4)

Fig. 1:   (a) The XRD partens of V-Mo$_2$C. (b) Raman spectra of V-Mo$_2$C and Mo$_2$C catalysts. XPS spectra of (c) Mo 3d, (d) C 1s, and (e) V 2p in the V-Mo$_2$C.

Therefore, NaHCO$_3$ was the carbon source in the synthesis of V-Mo$_2$C catalyst and the unreacted C was served as graphene. The feeding V/Mo ratio in V-MoO$_3$ precursor is 0.25. The V/Mo molar ratio in V-Mo$_2$C catalyst was probed by inductively coupled plasma optical emission spectrometer (ICP-OES) with the mass fraction values of 34.3 wt.% and 3.27 wt.% of Mo and V for V-Mo$_2$C catalyst, respectively. Therefore, it was calculated that about 2.88 wt.% of the carbon was used to form carbides and 59.55 wt.% to form graphene. As demonstrated in Fig 1b, the two Raman vibration modes at 1585 cm^{-1} and 1338 cm^{-1} are identified as the G-band and the D-band of carbon, respectively. The intensity ratio of the D to G bands (I$_D$/I$_G$) are 0.943 and 0.939 of Mo$_2$C and V-Mo$_2$C catalysts, respectively. This result indicates that the introduction of V atoms has little effect on the formation of graphene and the graphene is the amorphous carbon, which is consistent with the XRD results.The Mo 3d peak in V-Mo$_2$C (Fig. 1c) was fit into six peaks of Mo^{2+} 3d$_{5/2}$ (228.5 eV), Mo^{2+} 3d$_{5/2}$ (230.6 eV), Mo^{4+} 3d$_{5/2}$ (229.0 eV), Mo^{4+} 3d$_{3/2}$ (233.1 eV), Mo^{6+} 3d$_{5/2}$ (232.1 eV) and Mo^{6+} 3d$_{3/2}$ (235.7 eV) [30-31], demonstrating the composition of Mo$_2$C. From C 1s XPS spectrum in V-Mo$_2$C catalyst (Figure 2d), the peaks at 283.9 eV, 284.2 eV, 284.6 eV, 285.6 eV and 290.5 eV are assigned to C-V, C-Mo, C-C, C-O and O-C=O [32-33]. As demostated in Figure 1e, the high-resolution V 2p XPS spectra could be deconvoluted into four types of V species including V-C 2p$_{3/2}$(515.6 eV), V-C 2p$_{1/2}$(523.5 eV), V-O 2p$_{3/2}$(517.5eV), and V-O 2p$_{1/2}$ (525.1 eV).

The high-resolution transmission electron microscopy (HRTEM) was conducted and represented in Fig. 2. Mo$_2$C nanoparticles were anchoraged on graphene as shown in Fig. 2a, which emerges uniform sheets. This morphology can effectively increase the specific surface area of the electrocatalyst, thus exposing more active sites for HER. Fig. 2b,c reveals that Mo$_2$C nanoparticles are distributed on the surface of graphene uniformly with an average particle size of 2 nm (yellow arrows). The Mo$_2$C particles are no agglomeration and overgrowth, which is also beneficial to enhance the catalytic area of the electrocatalyst. The high-resolution HRTEM image shows the lattice fringe spacing of 0.20 corresponding to the (100) facet of Mo$_2$C. This result is consistent with the XRD analysis. Beyond that, we can clearly observe the graphene structure, which can effectively improve the conductivity of the catalyst and long-term stability. Fig. 2d shows a high-resolution scanning transmission electron microscope (STEM) image of the electrocatalyst obtained under the high-angle annular dark- field (HAADF) mode together with its corresponding energy-dispersive X-ray spectrometer (EDS) elemental mapping results. C, Mo, V elements are uniformly distributed. This phenomenon further confirmed the successful synthesis of ultrafine Mo$_2$C nanoparticles anchorage on graphene nanosheets.
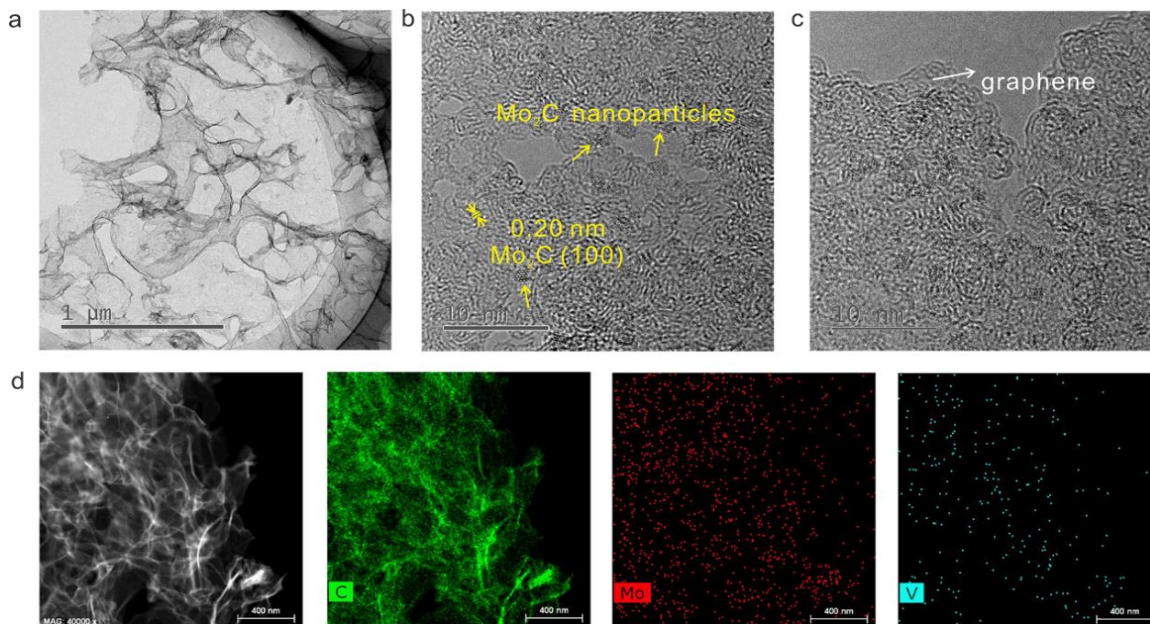
Fig. 2: (a) TEM image of V-Mo$_2$C. (b, c) HRTEM images of V-Mo$_2$C. (d) EDS elemental mappings distribution of V-Mo$_2$C.

The activities and kinetics of these samples were measured by polarization curve and corresponding Tafel plots in alkaline electrolyte, as illustrated in Fig. 3. The V-Mo$_2$C catalyst achieves the overpotentials of 284 mV in 1 M KOH at the current density of -10 mA·cm^{-2}, respectively (Fig. 3a), which is much lower than Mo$_2$C (600 mV). Furthermore, the corresponding Tafel slope of V-Mo$_2$C catalyst is 65.0 dec^{-1} in alkaline, followed by Mo$_2$C (121.1 dec^{-1}) as shown in Fig. 3b. These results demonstrate that V atoms can effectively tailor the electronic structure of catalysts. Moreover, combining ultrafine nanoparticles with ultrathin graphene substrate can obviously improve the HER performance of Mo$_2$C-based electrocatalyst. The stability test (Fig. 3c) was conducted at -0.284 V$_{RHE}$ for 24 h. The result shows that the current density decreases slightly in the subsequently hours. We conducted the characterization of the V-Mo$_2$C catalyst after HER test with TEM and XRD (the insets of Fig. 3c). The morphology of the V-Mo$_2$C catalyst after stability test in 1 M KOH remains similar with the fresh one (Fig. 3c(Ⅰ)). However, the crystallinity of the V-Mo$_2$C catalyst becomes worse after stability test in 1 M KOH (Fig. 3c(Ⅱ)). This is probably the reason of the poor durability of V-Mo$_2$C catalyst. As illustrated in Fig. 3d, the Nyquist plots of V-Mo$_2$C and Mo$_2$C catalysts were elucidated by electrochemical impedance spectroscopy (EIS). The inset of Fig. 3d is the equivalent circuit obtained by the tested EIS curve fitting. Note that, it is known that a smaller charge transfer resistance (R$_{ct}$) suggests a faster kinetics for HER, which can be obtained from the semicircles at low frequency region. The EIS curve of V-Mo$_2$C catalyst exhibited the smaller R$_{ct}$, indicating its superior HER kinetics. This could be ascribed to the graphene substrate and strong combination between Mo$_2$C nanoparticles and graphene.

The electrochemically active surface area (ECSA) is another crucial factor to assess the activity of an electrocatalyst, which is linearly dependent on the double layer capacitance (C$_{dl}$). Fig. 4a shows the cyclic voltammograms (CV) curves of the samples at different scan rates. Derived from CV, the C$_{dl}$ values of V-Mo$_2$C and Mo$_2$C catalysts were calculated to be 2.18 and 0.75 mF cm^{-2} (Fig. 4b), respectively. This phenomenon shows that ultrafine nanoparticles and ultra-thin graphene can significantly increase the active area of electrocatalysts, which can improve their catalytic activity and kinetics for HER. As illustrated in Fig. 4c, the ECSA-normalized LSV curves are utilized to highlight the intrinsic catalytic activity. It is obvious that the ECSA-normalized overpotential of V-Mo$_2$C is lower than that of Mo$_2$C at -0.2 mA cm^{-2}, suggesting that the higher HER activity of V-Mo$_2$C catalyst results from not only the increased ECSA but also the enhanced intrinsic catalytic activity. This can be attributed to the regulation of the electron structure of Mo$_2$C by V atoms. The calculated ECSA and roughness factors (R$_f$) are summarized in Fig. 4d. The V-Mo$_2$C catalyst demonstrates the largest ECSA and highest R$_f$, which could be ascribed to a large surface area, which induced by ultrafine nanoparticles and graphene sheets.
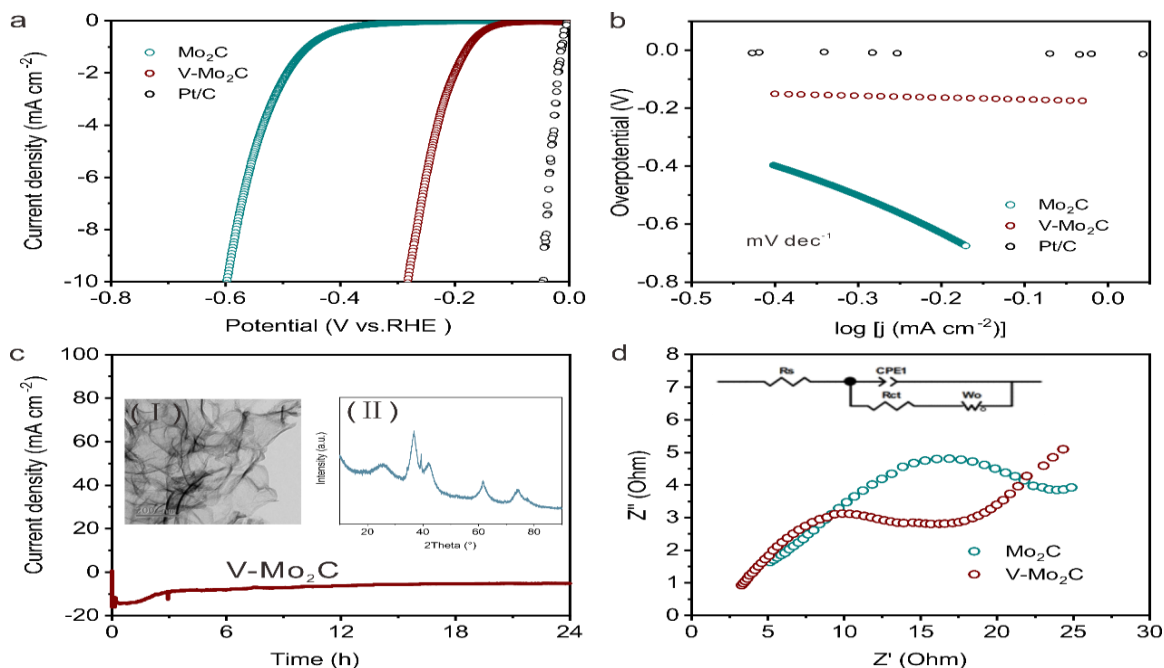
Fig. 3:   (a) LSV curves and (b) Tafel plots of the Pt, V-Mo₂C, and Mo₂C catalysts. (c) The stability test of V-Mo₂C test at -284mV over 24 h and the insets of Fig.3c are (I) the morphology and (II) XRD pattern of the V-Mo₂C catalyst after stability test. (d) The EIS curves of V-Mo₂C and Mo₂C catalysts. All the tests were conducted in 1 M KOH.
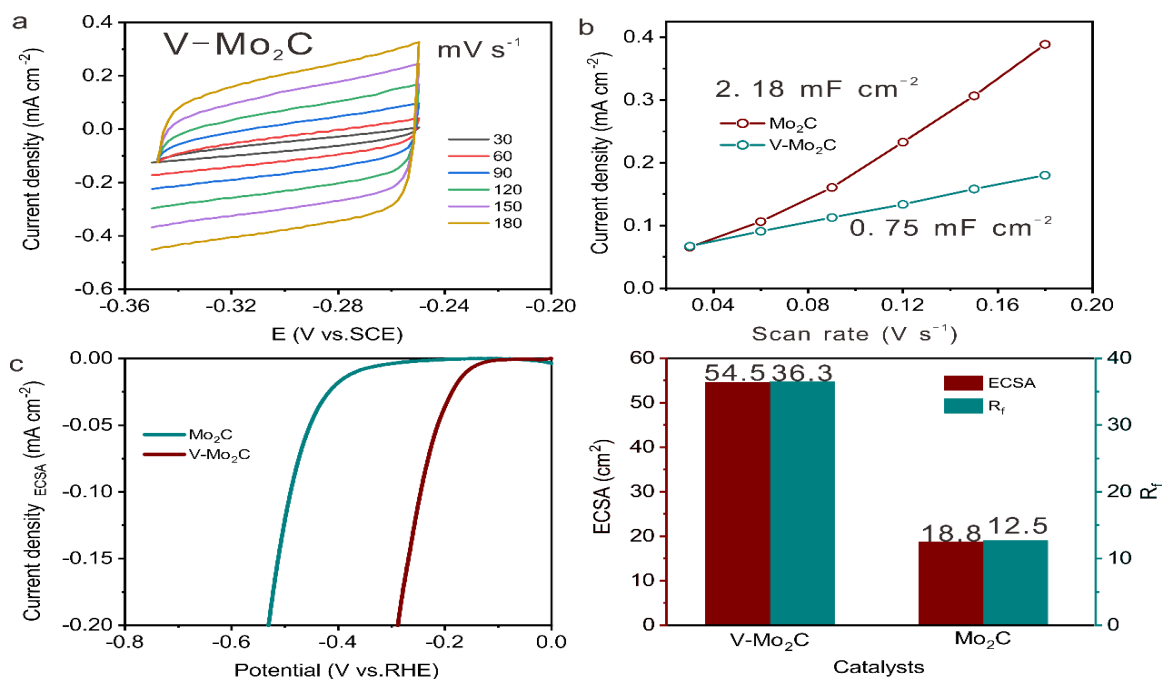

Fig. 4:   (a) CVs of the V-Mo₂C at different scan rates. (b) Plots for the C_{dl} of V-Mo₂C and Mo₂C. (c) The normalized LSV curves of V-Mo₂C and Mo₂C. (d) The ECSA and R_f values of V-Mo₂C and Mo₂C.

Conclusion

In summary, we demonstrate a facile, energy-saving strategy for the controllable synthesis of ultrafine V doped Mo_2C nanoparticles with the size of about 2 nm, which anchoraged on graphene. The overpotential of the as-prepared $V-Mo_2C$ catalyst is 284 mV at a current density of -10 mA cm^{-2} with an excellent stability. The corresponding Tafel slopes was only 65.0 dec^{-1}. The excellent HER performance can be ascribed to the following factors: (Ⅰ) V atoms doping can significantly regulate the electronic structure of Mo_2C, improving the intrinsic activity and the number of active sites of electrocatalyst for HER; (Ⅱ) The ultrafine Mo_2C nanoparticles with the size of about 2 nm are firmly anchoraged on conductivity graphene substrate, which increases the number of active sites and contributes the high HER activity. This work provides a facile and universal strategy for hybridizing ultrafine transition metal carbide and carbon-based supports for effective hydrogen generation or other catalytic systems.

Declaration of interest statement

No conflict of interest exists in the submission of this manuscript, and the manuscript is approved by all authors for publication.

References

1. H. Lin, N. Liu, Z. Shi, Y. Guo, Y. Tang, Q. Gao, Cobalt-Doping in Molybdenum-Carbide Nanowires Toward Efficient Electrocatalytic Hydrogen Evolution. *Adv. Funct. Mater.* **26**, 5590 (2016).

2. C. Tang, W. Wang, A. Sun, C. Qi, D. Zhang, Z. Wu, D. Wang, Sulfur-Decorated Molybdenum Carbide Catalysts for Enhanced Hydrogen Evolution. *ACS Catal.* **5**, 6956 (2015).

3. S. Jing, L. Zhang, L. Luo, J. Lu, S. Yin, P. K. Shen, P. Tsiakaras, One-Pot Synthesized Boron-Doped RhFe Alloy with Enhanced Catalytic Performance for Hydrogen Evolution Reaction. *Appl. Catal. B Environ.* **224**, 533 (2018).

4. D. Escalera-López, Z. Lou, N. V. Rees, Benchmarking the Activity, Stability, and Inherent Electrochemistry of Amorphous Molybdenum Sulfide for Hydrogen Production. *Adv. Energy Mater.* **9**, 1802614 (2019).

5. L. Schlapbach, L. Schlapbach, A. Züttel, Hydrogen-storage materials for mobile applications. *Nature.* **414**, 353 (2001).

6. J. Zhang, C. Zhang, Z. Wang, J. Zhu, Z. Wen, X. Zhao, X. Zhang, J. Xu, Z. Lu, Synergistic Interlayer and Defect Engineering in VS_2 Nanosheets toward Effcient Electrocatalytic Hydrogen Evolution Reaction. *Small*, **14**, 1703098 (2018).

7. X. Yang, A. Y. Lu, Y. Zhu, M. N. Hedhili, S. Min, K. W. Huang, Y. Han, L. J. Li, CoP nanosheet assembly grown on carbon cloth: A highly efficient electrocatalyst for hydrogen generation. *Nano Energy* **15**, 634 (2015).

8. J. Ekspong, T. Sharifi, A. Shchukarev, A. Klechikov, T. Wågberg, E. Gracia-Espino, Stabilizing active edge sites in semicrystalline molybdenum sulfide by anchorage on nitrogen-doped carbon nanotubes for hydrogen evolution reaction. *Adv. Funct. Mater.* **26**, 6766 (2016).

9. P. Zhuang, Y. Sun, P. Dong, W. Smith, Z. Sun, Y. Ge, Y. Pei, Z. Cao, P. M. Ajayan, J. Shen, M. Ye, Revisiting the role of active sites for hydrogen evolution reaction through precise defect adjusting. *Adv. Funct. Mater.* **29**, 1901290 (2019).

10. X. Zou, Y. Zhang, Noble metal-free hydrogen evolution catalysts for water splitting. *Chem. Soc. Rev.* **44**, 5148 (2015).

11. Z. Cai, Y. Bi, E. Hu, W. Liu, N. Dwarica, Y. Tian, X. Li, Y. Kuang, Y. Li, X. Q. Yang, H. Wang, X. Sun, Single-Crystalline Ultrathin Co3O4 Nanosheets with Massive Vacancy Defects for Enhanced Electrocatalysis. *Adv. Energy Mater.* **8**, 1701694 (2018).

12. J. Halim, S. Kota, M. R. Lukatskaya, M. Naguib, M. Q. Zhao, E. J. Moon, J. Pitock, J. Nanda, S. J. May, Y. Gogotsi, M. W. Barsoum, Synthesis and characterization of 2D molybdenum carbide (MXene). *Adv. Funct. Mater.* **26**, 3118 (2016).

13. Y. Li, K. Yin, L. Wang, X. Lu, Y. Zhang, Y. Liu, D. Yan, Y. Song, S. Luo, Engineering MoS2 nanomesh with holes and lattice defects for highly active hydrogen evolution reaction. *Appl. Catal. B Environ.* **239**, 537 (2018).

14. Z. Lv, M. Tahir, X. Lang, G. Yuan, L. Pan, X. Zhang, J. J. Zou, Well-dispersed molybdenum nitrides on a nitrogen-doped carbon matrix for highly efficient hydrogen evolution in alkaline media. *J. Mater. Chem. A* **5**, 20932 (2017).

15. J. Tian, Q. Liu, A. M. Asiri, X. Sun, Self-supported nanoporous cobalt phosphide nanowire arrays: an efficient 3D hydrogen-evolving cathode over the wide range of pH 0–14. *J. Am. Chem. Soc.* **136**, 7587 (2014).

16. S. Yuan, S. Xu, Z. Liu, G. Huang, C. Zhang, J. Ai,

X. Li, N. Li, Ultra-Small Molybdenum Carbide Nanoparticles in situ Entrapped in Mesoporous Carbon Spheres as Efficient Catalysts for Hydrogen Evolution. *ChemCatChem* **11**, 201900324 (2019).

17. M. Qamar, A. Adam, B. Merzougui, A. Helal, O. Abdulhamid, M. N. Siddiqui, Metal–organic framework-guided growth of Mo2C embedded in mesoporous carbon as a high-performance and stable electrocatalyst for the hydrogen evolution reaction. *J. Mater. Chem.* A. **4**, 16225 (2016).

18. Z. Cheng, Q. Fu, Q. Han, Y. Xiao, Y. Liang, Y. Zhao, L. Qu, A type of 1 nm molybdenum carbide confined within carbon nanomesh as highly efficient bifunctional electrocatalyst. *Adv. Funct. Mater.* **28**, 1705967 (2018).

19. R. Ma, Y. Zhou, Y. Chen, P. Li, Q. Liu, J. Wang, Ultrafine molybdenum carbide nanoparticles composited with carbon as a highly active hydrogen-evolution electrocatalyst. *Angew. Chemie - Int. Ed.* **54**, 14723 (2015).

20. J. F. Lin, O. Pitkänen, J. Mäklin, R. Puskas, A. Kukovecz, A. Dombovari, G. Toth, K. Kordas, Synthesis of tungsten carbide and tungsten disulfide on vertically aligned multi-walled carbon nanotube forests and their application as non-Pt electrocatalysts for the hydrogen evolution reaction. *J. Mater. Chem.* A. **3**, 14609 (2015).

21. Q. Gong, Y. Wang, Q. Hu, J. Zhou, R. Feng, P. N. Duchesne, P. Zhang, F. Chen, N. Han, Y. Li, C. Jin, Y. Li, S. T. Lee, Ultrasmall and phase-pure W 2 C nanoparticles for efficient electrocatalytic and photoelectrochemical hydrogen evolution. *Nat. Commun.* **7**, 13216 (2016).

22. Y. Shen, L. Li, J. Xi, X. Qiu, A facile approach to fabricate free-standing hydrogen evolution electrodes: riveting tungsten carbide nanocrystals to graphite felt fabrics by carbon nanosheets. *J. Mater. Chem.* A **4**, 5817 (2016).

23. L. F. Pan, Y. H. Li, S. Yang, P. F. Liu, M. Q. Yu, H. G. Yang, Molybdenum carbide stabilized on graphene with high electrocatalytic activity for hydrogen evolution reaction. *Chem. Commun.* **50**, 13135 (2014).

24. K. Zhang, C. Li, Y. Zhao, X. Yu, Y. Chen, Porous one-dimensional Mo 2 C–amorphous carbon composites: high-efficient and durable electrocatalysts for hydrogen generation. *Phys. Chem. Chem. Phys.* **17**, 16609 (2015).

25. W. F. Chen, C. H. Wang, K. Sasaki, N. Marinkovic, W. Xu, J. T. Muckerman, Y. Zhu, R. R. Adzic, Highly active and durable nanostructured molybdenum carbide electrocatalysts for hydrogen production. Energy *Environ. Sci.* **6**, 943 (2013).

26. X. Fan, Z. Peng, R. Ye, H. Zhou, X. Guo, M3C (M: Fe, Co, Ni) Nanocrystals Encased in Graphene Nanoribbons: An Active and Stable Bifunctional Electrocatalyst for Oxygen Reduction and Hydrogen Evolution Reactions. *ACS Nano*, **9**, 7407 (2015).

27. Z. Zhong, N. Liu, H. Chen, X. Fu, L. Yang, Q. Gao, Molybdenum carbide supported by N-doped carbon: Controlled synthesis and application in electrocatalytic hydrogen evolution reaction. *Mater. Lett.* **176**, 101 (2016).

28. B. Yu, D. Yang, Y. Hu, J. He, Y. Chen, W. He, Mo₂C Nanodots Anchored on N-Doped Porous CNT Microspheres as Electrode for Efficient Li-Ion Storage. *Small Methods*, **3**, 1800287 (2019).

29. X. Peng, L. Hu, L. Wang, X. Zhang, J. Fu, K. Huo, L. Y. S. Lee, K. Y. Wong, P. K. Chu, Vanadium carbide nanoparticles encapsulated in graphitic carbon network nanosheets: A high-efficiency electrocatalyst for hydrogen evolution reaction. *Nano Energy*, **26**, 603 (2016).

30. S. Jing, L. Zhang, L. Luo, J. Lu, S. Yin, P. K. Shen, P. Tsiakaras, N-doped porous molybdenum carbide nanobelts as efficient catalysts for hydrogen evolution reaction. *Appl. Catal. B Environ.* **224**, 533 (2018).

31. H. Huang, C. Yu, H. Huang, W. Guo, M. Zhang, X. Han, Q. Wei, S. Cui, X. Tan, J. Qiu, Microwave-Assisted Ultrafast Synthesis of Molybdenum Carbide Nanoparticles Grown on Carbon Matrix for Effcient Hydrogen Evolution Reaction. *Small Methods* **3**, 1900259 (2019).

32. C. Wu, D. Liu, H. Li, J. Li, Molybdenum Carbide-Decorated Metallic Cobalt@ Nitrogen-Doped Carbon Polyhedrons for Enhanced Electrocatalytic Hydrogen Evolution. Small **14**, 1704227 (2018).

33. C. Lu, D. Tranca, J. Zhang, F. Rodrĺguez Hernández, Y. Su, X. Zhuang, F. Zhang, G. Seifert, X. Feng, Molybdenum Carbide-Embedded NitrogenDoped Porous Carbon Nanosheets as Electrocatalysts for Water Splitting in Alkaline Media. *ACS Nano* **11**, 3933 (2017).